

Broad spectral photonic crystal fiber surface enhanced Raman scattering probe

Z. Xie · Y. Lu · H. Wei · J. Yan · P. Wang · H. Ming

Received: 28 September 2008 / Revised version: 12 January 2009 / Published online: 3 April 2009
© Springer-Verlag 2009

Abstract A broad spectral surface enhanced Raman scattering sensor is developed using the solid core holey photonic crystal fiber with silver nanoparticles cluster. This SERS probe offers an operational excitation wavelength range overlaying visible light and near infrared light. The PCF SERS sensing is demonstrated in the detection of the 4-Mercaptobenzoic acid (10^{-6} M) solution with 514.5 and 785 nm excitation. In this structure of PCF sensor, the related analysis shows that leakage modes also make an important contribution in the SERS activity not only by the evanescent field way.

PACS 82.80.-d · 07.07.Df · 42.81.-i

1 Introduction

In recent years, optical fiber surface enhanced Raman scattering (SERS) sensors [1–4] have gained increasing attention in chemical, biological, and environment detection due to the huge enhancement factor of SERS and the flexibility of optical fibers which are used to deliver the excitation laser and collect the Raman scattering signal. Various configurations such as end tip, taper tip and D-shaped have been developed as SERS substrates [5–7]. The main limitations

in these configurations are small active areas, thus requiring high laser intensities to get distinct Raman spectrum in vivo and in vitro application.

To increase the active area, photonic crystal fibers (PCF) are chosen to make the SERS probes [8, 9]. Filling air holes with metal nanoparticles and analyte molecules, only a sub-microliter of a liquid sample can provide larger active SERS area by the long interaction length. The hollow core PCF provides the strong interaction of field-particles because the excited power is confined in the core. But the operational wavelength suffers from the narrow transmission band, only certain wavelengths within the bandgap ranges are transmitted [10]. However, suitable excitation wavelength should be selected for reducing the damage to sample, and also for avoiding the disturbance of strong fluorescence background in Raman spectroscopy. For example, gallstones and kidney stones are investigated extensively using visible excitation because of the large Raman scattering cross-section and relatively weak fluorescence. Most biological tissues are suitable for the near-IR excitation due to reduced fluorescence emission and deep penetration [11].

The solid core PCF confines the light with total internal reflection mechanism, and a wide range of wavelength can be guided in the waveguide for transmission. In the previous reports [12, 13], the high pressure chemical deposition technique was used to deposit silver nanoparticles into the air hole cladding. It is not only complicated in manipulation, but also the transmission loss is huge, about 0.6–1 dB/cm, limiting the distance of optical fiber in application. In this paper, we present a broad spectral SERS sensor, consisting of a solid core photonic crystal fiber and silver colloid cluster. Silver colloids are easily prepared and manipulated. Not filling the total fiber with silver nanoparticles, we utilize the capillary effect to make a very short fiber part with silver

Z. Xie · Y. Lu (✉) · J. Yan · P. Wang · H. Ming
Anhui Key Laboratory Optoelectronic Science and Technology,
Department of Physics, University of Science and Technology
of China, Hefei, Anhui 230026, China
e-mail: yhlu@ustc.edu.cn
Fax: +86-551-3601745

H. Wei
Yangtze Optical Fibre and Cable Co., Ltd, Wuhan, Hubei 430073,
China

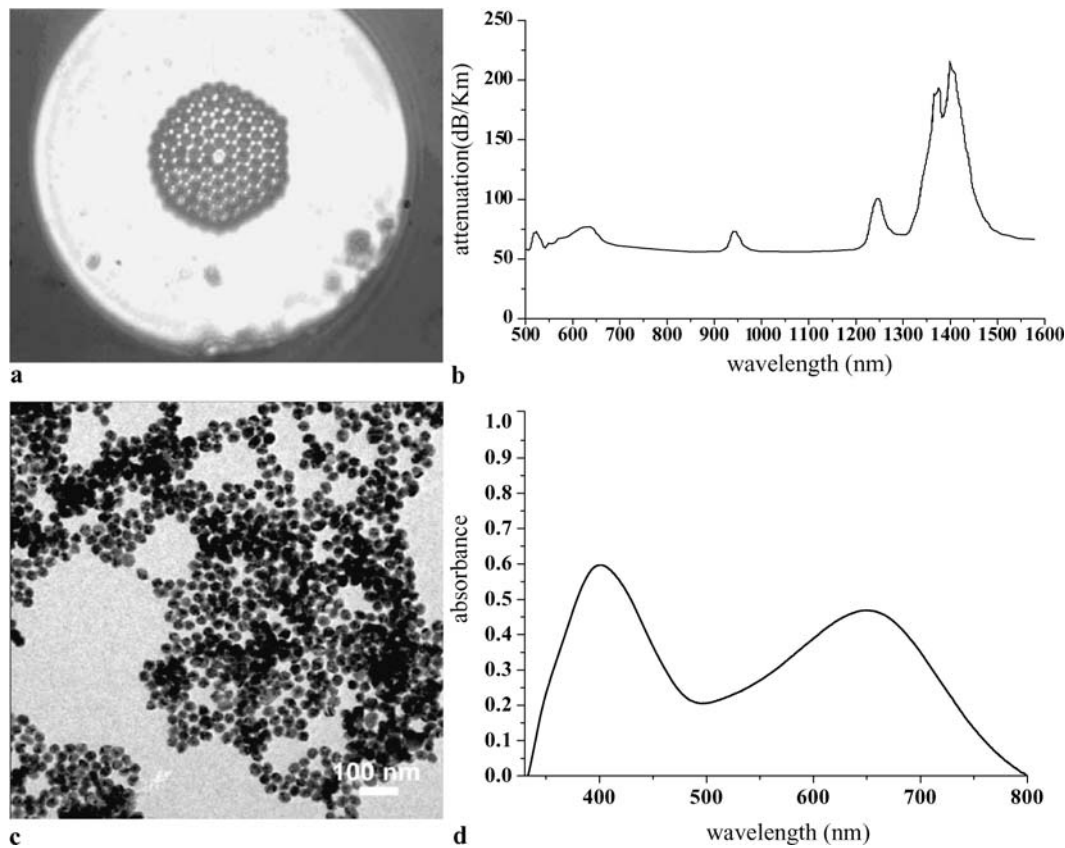


Fig. 1 (a) Micrographs of the cross-section of the holey photonical crystal fiber; (b) transmission spectrum of the solid core holey photonic crystal fiber; (c) TEM images of silver nanoparticles synthesized by microwave method; (d) the extinction spectrum of silver colloid cluster

nanoparticles. The longer fiber part is preserved to transmit the light and to collect the signal for the potential far distance application. Meanwhile, silver nanoparticles' cluster can produce broad plasmons band to offer a wide wavelength range for the enhancement of electromagnetic field, right across the visible region to the near-infrared [14].

2 Experiment

The PCF is fabricated by China YOFC Company Ltd. Fig. 1(a) shows the cross-section of the solid core holey PCF. It is made of pure-silica with a triangular lattice of air holes whose diameter and pitch are 2.7 and 3 μm , respectively. In the center, an air hole is omitted to create the defect of high refractive index. The total diameter including the outer coating is 80 μm . This waveguide possesses good performance of transmission from visible light to near-infrared light as illustrated in Fig. 1(b), making it suitable for broad spectral application. In the experiment, the PCF is cut into 10 cm segment with both ends cleaved carefully. Silver colloid cluster is prepared by the method of microwave assisted “green” synthesis [15], and the transmission electron microscope image shows that the mean diameter of silver

nanoparticle is about 15 nm and mass nanoparticles assemble together in Fig. 1(c). The absorption spectrum of the silver colloid cluster in Fig. 1(d) indicates two plasmon bands corresponding to the silver nanosphere and the aggregation of silver nanospheres, respectively.

As shown in Fig. 2, a 50 \times microscope objective lens is used to couple the excitation laser into the PCF, and the backscattering SERS signal is also collected by objective lens into the Raman spectrometer Ramanlog 6. The coupling between the objective lens and the fiber is carefully calibrated to eliminate the loss as much as possible. A continuous-wave Ar-ion laser (514.5 nm) and a diode laser (785 nm) are used as excitation source to verify the broad spectral characteristic of the SERS probe. During the measurement, the probing tip is dipped into the mixed solution of 0.1 mL 4-MBA (10^{-5} M) and 0.9 mL silver colloid, allowing the solution to fill the cladding air holes of about 1 cm length by capillary effect. It is reasonable to assume that the silver colloid cluster keeps its broadband plasmon absorption within the air hole of PCF because the clusters are very small and the normalized absorption changes little in the period of experiment after being mixed with analyte solution. The molecule SERS spectrum is obtained by visible light of 514.5 nm with 0.3 mW power, and scan time of

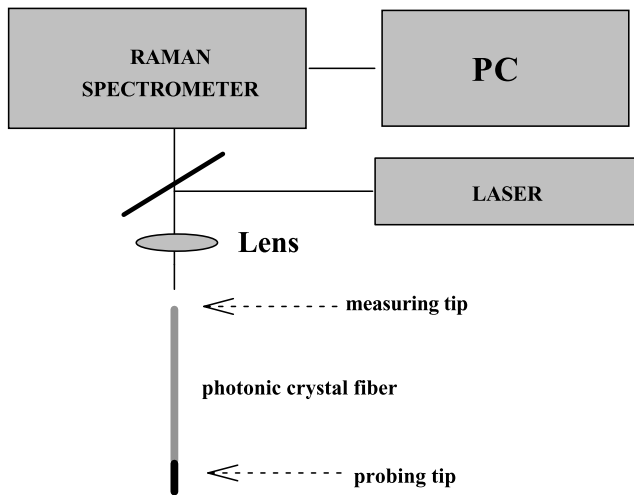


Fig. 2 A schematic diagram of the experiment setup

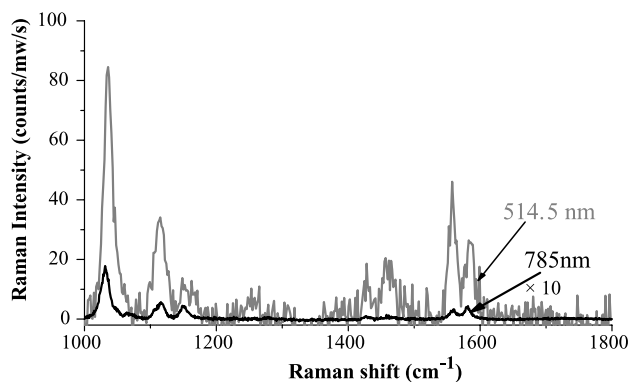


Fig. 3 Raman spectrum obtained from 4-MBA with silver nanoparticles, excited by a 514.5 nm and a 785 nm laser. SERS spectra have been background corrected, and shifted to have a baseline close to zero

90 s. The SERS sensing is carried out in near-infrared wavelength of 785 nm with 3 mW power, and scan time of 90 s. SERS spectra have been background corrected and shifted to have a baseline close to zero. Visible excitation SERS and near-IR excitation SERS are demonstrated in Fig. 3. The molecule Raman characteristic peaks are consistent in both excitation light, and the SERS peak positions are also the same as in the literature [16]. To clarify that what we detected are the SERS signals rather than regular Raman signals, the same length PCF is dipped in the 4-MBA (10^{-6} M) solution without silver colloid. The regular Raman signal is measured, and no molecules' Raman peaks are observable in both light excitation. To assess the repeatability of our results, we measure a batch of fibers in the identical manner. All results produce similar intensities of the SERS peaks.

3 Results and discussion

The broad spectral excitation properties of the SERS experiment is ensured not only by the wide transmission band of the PCF but also by the wide plasmon absorption band of the silver cluster. In Fig. 1(d), spherical silver particles' plasmon resonance occurs at 400 nm, and the cluster of silver nanoparticles induces a red shifted and broad plasmon resonant band. In such colloidal cluster structures, the individual plasmons of the small isolated particles cause the coupling of plasmon modes. Therefore, the local field excitation distributes very inhomogeneously over the entire cluster, tends to have spatially localized 'hot' areas and strongly depends on the excitation wavelength [17]. In the experiment, the plasmons' band absorption at 514.5 and 785 nm is from the silver cluster. The SERS spectrum in 785 nm light excitation is weaker than that in 514.5 nm light excitation in Fig. 3. According to the formula $I_{\text{SERS}}(\nu_S) = N\sigma_{\text{SERS}}|A(\nu_L)|^2|A(\nu_S)|^2I(\nu_L)$, SERS signal intensities depend on the excitation wavelength and the local electromagnetic field if only electromagnetic enhancement mechanism is considered. N is the number of molecules which are involved in the SERS process, σ_{SERS} describes the Raman cross-section, which is λ^{-4} dependence, $A(\nu_L)$ and $A(\nu_S)$ express enhancement factors for the laser and for the Raman scattered field, respectively. The calculation is complicated for this excitation-wavelength-dependent enhancement. Previous theoretic and experimental works [18, 19] indicate the profiles of the SERS enhancement should follow the trend of the secondary plasmons resonance on statistical average. So, we can imagine that a broad spectral SERS sensor from the visible to the near infrared can be achieved. In fact, the SERS activity in the optical fiber structure, the exciting and collecting efficiency can also influence the signal intensities as we will discuss in the following.

Generally, the excitation light is confined to the core to propagate in the solid core PCF. As discussed widely in the literature [20, 21], the evanescent field plays an important role in SERS activity. In the exciting process of SERS, the evanescent field of guide modes spreads into the cladding to interact with metal nanoparticles. In the collecting process of Raman signal, the light from cladding cannot be trapped as guided core modes in terms of ray optics, but they can interact with the evanescent field tails of the guided core modes and transfer some of their power to guided core modes [22]. Although the evanescent field is a low efficient way, it is compensated by long SERS activity section.

In our experiment configuration, it is valuable to point out an important contribution of the leakage modes to SERS. The SERS probe can be divided into two different parts in the view of waveguide property, the air hole cladding part and the aqueous holes cladding part, when the probing tip is filled with aqueous solution. The commercial software

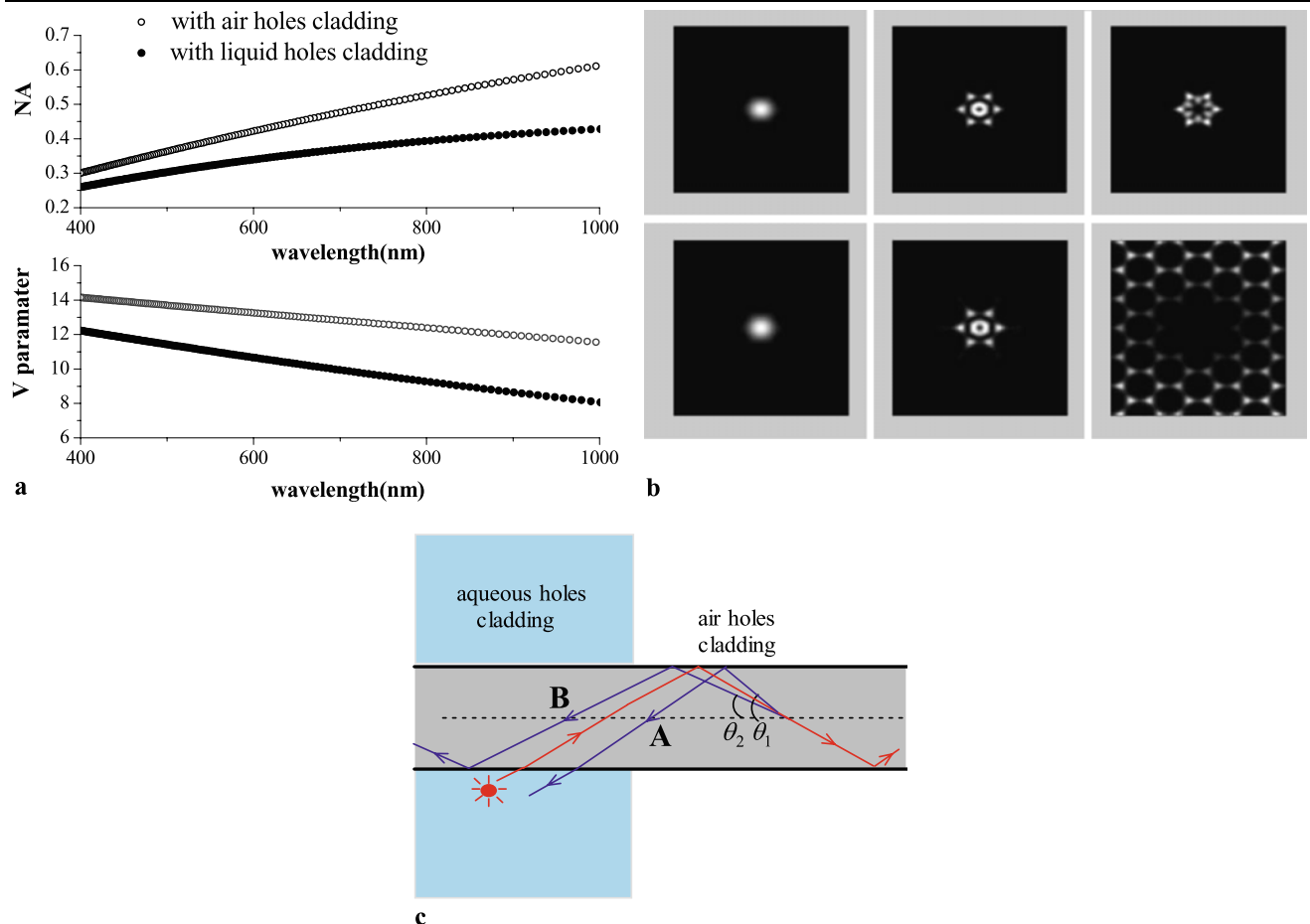


Fig. 4 (a) The numerical aspect NA (*upper*) and the V parameter (*lower*) versus light wavelength, *hollow circle* for air hole cladding, *solid circle* for liquid hole cladding; (b) some mode profiles with air hole cladding (*upper*) and liquid hole cladding (*lower*), the order of

mode $m = 1, 16, 21$ from left to right; (c) the light in the core leaks out to the fiber cladding, and the light in the cladding is guided in the core in geometric optical view

Bandsolve with plane-wave expansion method is used to simulate. Figure 4(a) shows the numerical aperture NA (upper) and the V parameter (below) with light wavelength. The liquid holes' cladding results in the decrease of NA and V parameter, which means that some high-order guide modes in air holes' cladding will leak into the aqueous holes' cladding, while propagating into the probing tip. Figure 4(b) shows the modes' field evolvement for both air holes' cladding (upper row) and aqueous holes' cladding PCF (lower row) in mode order of $m = 1, 16, 21$ (from left to right). For some low order modes such as $m = 1, 16$, optical fields are confined within the fiber core for both air and aqueous holes' cladding, and the evanescent field in the cladding can attribute to SERS activity. For the high order modes like $m = 21$, the leakage optical field in the aqueous holes will be involved in the SERS activity. In a simple but helpful geometric optical view in Fig. 4(c), the light with an angle range $0 \leq \theta \leq \theta_1$ is guided in the fiber core to propagate in the part with air holes' cladding, where θ_1 is

the complementary angle of the critical total reflection between the fiber core and the cladding of air holes, labeled as light line A, about 14.69° at 514.5 nm and 20.87° at 785 nm from the modeling result Fig. 4(a). When coming into the part with aqueous holes' cladding, only light with an angle $0 \leq \theta \leq \theta_2$ is still confined, θ_2 being the complementary angle of the critical total reflection between the fiber core and the cladding of aqueous holes, marked as light line B, about 11.87° at 514.5 nm and 15.51° at 785 nm. The light with an angle $\theta_2 \leq \theta \leq \theta_1$ will leak out of the fiber core to interact with metal nanoparticles; here it accounts for 19.2% at 514.5 nm and for 25% at 785 nm in the total power of excitation light, assuming equal power distribution on the angle. In Raman signal collecting process, the beams can penetrate into the higher-index core region from the lower-index cladding with an angle range $\theta_2 \leq \theta \leq 90^\circ$, it cannot be confined in the core and will reflect several times back to the cladding. However, the beams with an angle $\theta_2 \leq \theta \leq \theta_1$ will be confined in the fiber core when passing back the air holes

segment; about 0.9% of Raman scattering light at 514.5 nm and 1.8% at 785 nm is collected when considering all Raman scattering directions. There are more excitation beams to leak out and more signals to be collected in longer wavelength. But it does not indicate that the longer wavelength is good at SERS signal intensity because the SERS activity is related to excitation wavelength and plasmons band.

4 Conclusion

We present a broad spectral SERS sensor based on solid core photonic crystal fiber with silver colloid cluster. The PCF SERS platform to detect 4-MBA molecules is demonstrated with visible light of 514.5 nm and near-infrared light of 785 nm. Excellent and consistent SERS spectrums are obtained. Furthermore, the exciting process of SERS and the collecting process of Raman signal on solid core photonic crystal fiber is discussed. Besides the low efficient way of the evanescent field, leakage modes create important action in the solid core PCF SERS probe.

Acknowledgements This work is supported by the National Key Basic Research Program of China No. 2006CB302905, the Key Program of National Natural Science Foundation of China No. 60736037, the National Natural Science Foundation of China No. 10704070 and the Science and Technological Fund of Anhui Province for Outstanding Youth.

References

1. J.Y. Ma, Y.S. Li, *Appl. Spectrosc.* **48**, 1529 (1994)
2. D.L. Stokes, T. Vo-Dinh, *Sens. Actuators, B, Chem.* **69**, 28 (2000)
3. D.L. Stokes, Z.H. Chi, T. Vo-Dinh, *Appl. Spectrosc.* **58**, 292 (2004)
4. D.J. White, P.R. Stoddart, *Opt. Lett.* **30**, 598 (2005)
5. Y. Zhang, C. Gu, A.M. Schwartzberg, J.Z. Zhang, *Appl. Phys. Lett.* **87**, 123105 (2005)
6. H.Y. Chu, Y.J. Liu, Y.W. Huang, Y.P. Zhao, *Opt. Express* **15**, 12230 (2007)
7. S.J. Jia, S.P. Xu, X.L. Zheng, B. Zhao, W.Q. Xu, *Chem. J. Chin. Univ.* **27**, 523 (2006)
8. H. Yan, C. Gua, C.X. Yang, J. Liu, G.F. Jin, J.T. Zhang, L.T. Hou, Y. Yao, *Appl. Phys. Lett.* **89**, 204101 (2006)
9. Y. Zhang, C. Shi, C. Gu, L. Seballos, J.Z. Zhang, *Appl. Phys. Lett.* **90**, 193504 (2007)
10. J.C. Knight, *Nature* **424**, 847 (2003)
11. E.B. Hanlon, R. Manoharan, T.W. Koo, K.E. Shafer, J.T. Motz, M. Fitzmaurice, J.R. Kramer, I. Itzkan, R.R. Dasari, M.S. Feld, *Phys. Med. Biol.* **45**, R1 (2000)
12. A.C. Peacock, A. Amezcu-Correa, J. Yang, P.J.A. Sazio, S.M. Howdle, *Appl. Phys. Lett.* **92**, 141113 (2008)
13. A. Amezcu-Correa, J. Yang, C.E. Finlayson, A.C. Peacock, J.R. Hayes, P.J.A. Sazio, J.J. Baumberg, S.M. Howdle, *Adv. Funct. Mater.* **17**, 2024 (2007)
14. W.E. Smith, *Chem. Soc. Rev.* **37**, 955 (2008)
15. B. Hu, S.B. Wang, K. Wang, M. Zhang, S.H. Yu, *J. Phys. Chem. C* **112**, 11169 (2008)
16. Y. Imai, Y. Tamai, Y. Kurokawa, *J. Sol-Gel Sci. Technol.* **11**, 273 (1998)
17. V.A. Markel, V.M. Shalaev, P. Zhang, W. Huynh, L. Tay, T.L. Haslett, M. Moskovits, *Phys. Rev. B* **59**, 16 (1999)
18. M. Muniz-Miranda, G. Cardini, V. Schettino, *Theor. Chem. Acc.* **111**, 264 (2004)
19. J.A. Creighton, C.G. Blatchford, M.G. Albrecht, *J. Chem. Soc. Faraday Trans. 2* **75**, 790 (1979)
20. Y. Zhu, H. Du, *Opt. Express* **14**, 3541 (2006)
21. H. Yan, J. Liu, C. Yang, G. Jin, C. Gu, L. Hou, *Opt. Express* **16**, 8300 (2008)
22. D. Marcuse, *J. Lightw. Technol.* **6**, 1273 (1988)